Lysosomotropic cationic drugs induce cytostatic and cytotoxic effects: role of liposolubility and autophagic flux and antagonism by cholesterol ablation

Alexandre Parks, François Marceau

Axe Maladies Infectieuses et Immunitaires, CHU de Québec-Université Laval, Québec QC, Canada G1V 4G2;

Correspondence:

F. Marceau
CHU de Québec
Axe Maladies Infectieuses et Immunitaires, CHU de Québec-Université Laval, T1-49
2705 Laurier Blvd., Québec (Québec)
Canada G1V 4G2
Tel. 1-418-525-4444 ext. 46155
Fax: 1-418-654-2765
e-mail: francois.marceau@crchul.ulaval.ca

Abstract

Cation trapping in acidic cell compartments determines an antiproliferative effect that has a potential interest in oncology, as shown by clinical data and trials involving chloroquine and hydroxychloroquine. To further characterize the mechanism of this effect, we studied a series of 6 substituted triethylamine (s-Et_3N) drugs that encompasses a wide range of liposolubility (amiodarone, quinacrine, chloroquine, hydroxychloroquine, lidocaine, and procainamide). Three tumor cell lines and primary human endothelial cells were exploited in proliferation assays (48 hrs, cell counts). Accumulation of the autophagic effector LC3 II and the apoptotic marker cleaved PARP1 (immunoblots), cytotoxicity, cell cycle analysis and endocytic function were further tested in the p53-null histiocytic lymphoma U937 line. A profound and desynchronized antiproliferative effect was observed in response to all s-Et_3Ns with essentially no cell type specificity. Predictors of s-Et_3N potency were liposolubility and the acute accumulation of the autophagic effector LC3 II (6 hr-treatments). For each s-Et_3N, there was an antiproliferative concentration range where cytotoxicity and apotosis were not triggered in U937 cells (24-48 hr-treatments). Quinacrine was the most potent cytostatic drug (1-5 μM). Co-treatment of cells with inhibitors of cholesterol, β-cyclodextrin or lovastatin, partially reversed the antiproliferative effect of each s-Et_3N. The cytopathology induced by cationic drug accumulation includes a cytostatic effect. Its intensity is cell type- and p53-independent, but predicted by the inhibition of autophagic flux and by the liposolubility of individual drugs and alleviated by cholesterol ablation. The superiority of quinacrine, biomarker value of LC3 II and antagonism by a statin may be clinically relevant.

Keywords: lysosomotropic drugs; quinacrine; antiproliferative effect; cation trapping; autophagic flux.

Introduction

Lysosomotropic drugs can be defined as a series of weak bases that concentrate in acidic organelles, primarily the lysosomes and late endosomes, following their protonation at low pH and slow retrodiffusion under their cationic form; the proton pump V-ATPase provides the energy for this pseudo-transport mechanism (Marceau et al., 2012). The interruption of autophagosome clearance ensues in cells, and an antiproliferative effect is observed. A novel field of application of autophagic flux inhibitors is clinical oncology: hydroxychloroquine currently undergoes clinical trials for various solid and hematologic cancers (Sehgal et al., 2015). Chloroquine combination with conventional chemotherapy increased survival in patients with glioblastoma multiforme (Briceno et al., 2007). However, autophagy has context-dependent roles in cancer development and may be protective, especially early in the course of the disease (Thoburn et al., 2014).

Despite these exciting developments, little is known about the mechanisms and determinants of the anti-proliferative action of autophagic flux inhibitors. A constant feature of the cytopathology induced by cation accumulation in acidic vacuoles is an inhibition of cell proliferation without important cytotoxicity; we have observed this in various cellular models in response to lidocaine (Bawolak et al., 2010); 2-dimethylaminoethanol (Morissette et al., 2007), triethylamine (Et_3N) and procainamide (Morissette et al., 2004; 2005), as well as tamoxifen in an estrogen receptor-negative cell line (Marceau et al., 2012). Golden et al. (2015) recently analyzed the cytotoxic effect of a series of anti-malarial drugs: all were autophagic flux inhibitors of varying potency and

they induced apoptosis in human glioma cell lines independently of p53. Phospholipidosis is the late cytopathologic reorganization of vacuoles that have sequestered cationic drugs; in the affected cells, several genes that control lipid synthesis are upregulated (Sawada et al., 2005; Nioi et al., 2007). A new hypothesis about the antiproliferative effect of a lysosomotropic drug emerged in studies of leelamine, a novel lipophilic cationic agent: vacuolar cholesterol accumulation and interruption of vesicular cycling were observed (Kuzu et al., 2014). Cholesterol extraction using β-cyclodextrin reversed the antiproliferative effect and the depression of vacuolar traffic in that study.

We hypothesized that the antiproliferative effect of lysosomotropic drugs (1) is a universal response to amines susceptible to ion trapping; (2) possesses a uniform mechanism, mainly cytostatic and related to vacuolar alterations, and (3) exhibits a potency inversely correlated to their lipophilicity, as this physicochemical property clearly predicts the concentrations for which the cytopathology is observed (Marceau et al., 2012). To address these issues, we exploited a previously defined series of substituted triethylamine (s-Et_3N) drugs that span the whole lipophilicity scale (Suppl. Fig. 1) and that all were shown to be concentrated in a V-ATPase-dependent manner (Marceau et al., 2012). They include presently or formerly clinically used therapeutic agents but in classes that bear no obvious relationship with oncology (3 anti-malarial, 2 anti-arrhythmic and one local anesthetic drugs). Cell models used in the analysis were selected to isolate any cell-type specific effects; further, the mechanism of antiproliferative effects was characterized in a p53-null histiocytic lymphoma cell line.

Methods

Cell culture

The human melanoma M21 cell line, originally obtained from Dr. David Cheresh (The Scripps Research Institute, San Diego, CA), was a gift from Dr. Eric Petitclerc (Héma-Québec, Québec, Canada); it is tumorigenic in immunodeficient mice (McMahon et al., 2001). Most melanoma cells are extremely radioresistant and typically express non-mutated p53 protein; DNA-damaging agents lead to accumulation of p53 but not to apoptosis in these cells, as modeled by the M21 line (Bao and Strömblad, 2004). M21 and HEK 293a cells, originally obtained from Sigma-Aldrich, were cultured in DMEM supplemented with 5 and 10% fetal bovine serum, respectively, and antibiotics. The institutional research ethics board approved the anonymous use of human umbilical cord segments obtained after caesarean sections. Human umbilical vein endothelial cells (HUVECs) were isolated by collagenase digestion of umbilical veins from undamaged sections of fresh cords and cultured as described (Koumbadinga et al., 2010). The cells were maintained and passaged in Endothelial Cell Growth Medium (EGM, Lonza-Clonetics, Basel, Switzerland) used with the supplied growth supplement (final fetal bovine serum concentration 2%) and antibiotics. HUVECs express functional p53 (Zhang et al., 2011). Human monocytic leukemia cells (U937) were originally isolated from the histiocytic lymphoma of a 37-year-old male patient and were grown in RPMI 1640 medium (GIBCO) supplemented with 10% fetal bovine serum. They are p53 null due to a large deletion in both copies of the *p53* gene (Shiohara et al., 1994; Oliveiro et al., 1997).

Cell proliferation and counting

The study of the antiproliferative effects of s-Et_3N drugs was made utilizing a previously applied proliferation assay in cellular models. Fifty thousand cells were plated with 2 mL of their respective culture medium in cell culture dish 35 mm (Starstedt) at time zero. Twenty-four hours afterwards, various concentrations of the cationic drugs were introduced. No change in the culture medium was made. At time 72-hrs, the cells were rinsed and detached with Trypsin+EDTA (ThermoFisher Scientific), except for the non-adherent U937 cells, and counted using the Cellometer® Mini (Nexcelom Bioscience, Lawrence, MA). The device and associated software were used precisely as directed. Six s-Et_3N drugs were tested for their antiproliferative effects; amiodarone, chloroquine, hydroxychloroquine, lidocaine, procainamide and quinacrine. Four cell lines were used for this proliferation assay; the HEK 293a cell line, the human melanoma M21 cell line, the human monocytic leukemia cells (U937) and umbilical vein endothelial cells (HUVECs).

A modified proliferation assay where 50,000 U937 cells were seeded along with s-Et_3N drugs and a co-treatment designed to probe the role of lipids of the mevalonate pathways in the antiproliferatice effects. These co-treatments consisted of β-cyclodextrin 1 mM, lovastatin 100 nM or geranylgeranyl-pyrophosphate 10 μM (all from Sigma-Aldrich). The cells were cultured for 48 hrs without washing and counted at the end of the incubation period.

Microscopy

The subcellular distribution of quinacrine in cultured human monocytic leukemia cells (U937) was monitored after treatments of 0-3 hrs at 37°C. Cells were incubated at 37°C in Eppendorf Thermomixer at a concentration of 1×10^6 cells per mL. Optional pre-treatment with bafilomycin A1, 100 nM for 30 min, was followed by incubation with quinacrine. After treatment, the cells were centrifuged at 12,500 RPM for 30 s at room temperature followed by removal of the supernatant. Cells were resuspended in 1 ml Hank's balanced salt solution (HBSS) pre-heated at 37°C to rinse the cells, then centrifuged again (same settings), and finally resuspended in 25 μl of RPMI 1640 medium. Five μl of the suspension were placed on a microscope slide and was photographed using Olympus BX51 microscope coupled to a CoolSnap HQ digital camera (transmission and fluorescence; filters for quinacrine's fluorescence: excitation 460-500 nm, emission 510-560 nm).

Cytofluorometry

Suspensions of 1×10^6 U937 cells were treated with fluorescent quinacrine for 1 hr or 48 hrs in their regular culture medium. Pre-treatment with bafilomycin A1 100 nM was applied 30 min before 1 h treatment with fluorescent drug. Optional co-treatment with β-cyclodextrin 1mM or lovastatin 100 nM was applied alongside the 48 hrs treatment of the fluorescent drug quinacrine. After treatments, the cells were centrifuged at 12,500 RPM for 30 s at room temperature followed by removal of the supernatant. Cells were resuspended in 1 mL of HBSS pre-heated at 37°C to rinse the cells, centrifuged again

(same settings), and resuspended in 250 µL of Hank's buffer pre-heated at 37°C. The cells were then submitted to cytofluorometric analysis of the uptake of quinacrine (green fluorescence) as described in Roy et al., (2013) using the BD SORP LSR II cell analyzer, BD Biociences (Franklin Lakes, NJ; fluorescence settings for FITC). In other experiments described below, it was possible to simultaneously record the green fluorescence of quinacrine along with that of other markers with different spectra of excitation/emission (Ex/Em).

To evaluate cytotoxicity, suspensions of 1×10^6 U937 cells were treated with the various s-Et_3N for 24 hrs or 48 hrs in their regular culture medium. After treatments, approximately 50,000 cells were harvested and centrifuged at 12,500 RPM for 30 s at room temperature. One ml of HBSS pre-heated at 37°C was added to rinse the cells. Then, the cell impermeant DNA stain DRAQ7 (Cell Signaling Technology) was added at a concentration of 3 µM. The cells were incubated with DRAQ7 for 2 min at 37°C in an Eppendorf Thermomixer at 350 RPM. After treatment, cells were analysed as directed (Ex/Em: 646/681 nm).

To analyze the cell cycle, suspensions of 1×10^6 U937 cells or cultured HUVEC, confluent at 80%, were treated with the various s-Et_3N for 48 hrs. After treatments, both types of cells were incubated for 1 hr at 37°C with Hoechst 33342 (10 µg/ml; Sigma-Aldrich). Afterwards, HUVECs were detached with Trypsin+EDTA (ThermoFisher Scientific), while approximately 300,000 U937 cells were harvested. Both type of cells

were centrifuged (12,500 RPM for 30 s for the U937 cells, and 1,200 for 5 mins for HUVECs) at room temperature followed by removal of the supernatant. Cells were resuspended in 1 ml of HBSS pre-heated at 37°C, centrifuged again (same settings) and resuspended in 250 µl of Hank's buffer pre-heated at 37°C. The cells were then submitted to cytofluorometric analysis as directed (Ex/Em: 346/460 nm).

To evaluate the endocytic function, suspensions of 1×10^6 U937 cells were treated with the various s-Et_3N for 24 hrs with optional co-treatment with β-cyclodextrin (1 mM). After treatments, approximately 200,000 cells were harvested and incubated in an Eppendorf Thermomixer at 350 RPM for 15 mins with transferrin-AlexaFluor-594 at 37°C. Afterwards, cells were centrifuged at 12,500 RPM for 30 s at room temperature followed by removal of the supernatant. Cells were resuspended in 1 ml of HBSS pre-heated at 37°C, centrifuged again (same settings), and resuspended in 250 µl of Hank's buffer pre-heated at 37°C. The cells were then submitted to cytofluorometric analysis as directed (Ex/Em: 590/617 nm).

Immunoblots

The analysis based on cultured human monocytic leukemia cells (U937) was established using a slight variation of a technique previously applied to a different cell type (Parks et al., 2015). Briefly, extracts of equal numbers (3×10^5) of non-adherent U937 cells were made as in Roy et al. (2013). Cells had been treated for 6 hrs with various drugs to monitor the effect on the autophagic protein LC3B. Extracts of 3×10^5 cells were run on a

15 % SDS-PAGE and transferred to a PVDF membrane. Anti-human LC3B rabbit polyclonal antibodies (Novus; dilution 1:3,000) were used to observe the effect on the cytosolic form LC3 I (18 kDa) and the lipidated and membrane-bound form LC3 II (16 kDa) (Morissette et al., 2008). Furthermore, to study the effects of various drugs on a late apoptotic reaction mediated by caspase-3, the polyclonal rabbit anti-poly(ADP-ribose)-polymerase I (-PARP1) antibody was used to monitor the cleavage of the latter protein (Cell Signalling, cat. #9542, dilution 1:1,000). In addition, three other cell types were tested for their autophagic and lysosomogenesis baselines. The human melanoma M21 cell line, HEK 293a cells and HUVEC lysates were centrifuged at 15,000 g for 5 minutes and incubated for 5 min at 95°C. To separate constituents from samples subsequently revealed using antibodies specific for p62/SQSTM1, LAMP1, P53, and β-actin a 9% SDS-PAGE was used. The lysosomal/late endosomal glycoprotein LAMP1 was detected in total cell extracts using the mouse monoclonal antibodies H4A3 (dilution 1:1,000, Developmental Studies Hybridoma Bank, Iowa City, IA) revealed using an HRP-conjugated anti rat IgG. p62/SQSTM1 rabbit monoclonal antibodies were from Cell Signaling Technology (dilution 1:1000; cat. No. 5114). The mouse monoclonal anti-p53 antibodies (clone BP53-12, cat. No. P5813) were obtained from Sigma with used at a dilution of 1:1,000. The phosphorylated and non-phosphorylated forms of the retinoblastoma protein (pRB) were analysed using the rabbit monoclonal anti-phospho-pRB, $Ser^{807/811}$, and the mouse anti-pRB clone 4H1 (dilutions 1:1000 and 1:2000, respectively). Both these antibodies were also from Cell Signaling Technology (cat. No. 8516 and 9309 respectively). Equal track loading was verified by separating and transferring the same samples separately and immunoblotting for β-actin (mouse

monoclonal from Sigma-Aldrich, dilution 1:50,000). All reactions involved HRP-labelled secondary antibodies revealed using a luminescent substrate used as directed (Western Lighting, PerkinElmer) with CL-X Posure film (Thermo Scientific).

Cholesterol determination in U937 cells

Cholesterol determination (total and free cholesterol) was made with the help of the Cholesterol Quantitation Kit from Sigma-Aldrich (cat. No. MAK043). The kit was used precisely as directed. Briefly, 1×10^6 U937 cells were cultivated after 48 hrs treatment with various s-Et_3N. Lipids were extracted using chloroform:isopropanol:IGEPAL CA-630 (7:11:0.1) solution. Samples were then centrifuged at 13,000 g for 10 min at room temperature to remove any insoluble material. The supernatant was then transferred to a clean Eppendorf tube (1.5 ml). The lipids were then air dry at 50°C to remove any of the chloroform and any residue of organic solvent. The lipid pellets were then dissolved with the Cholesterol Assay Buffer provided in the kit. The cholesterol concentration was analysed using a black 96 well flat-bottom plate and compared to a cholesterol standard curve of 0, 0.1, 0.2, 0.3, 0.4 and 0.5 ng/well using the fluorometric detection steps of the kit. The samples and standards were analysed using TECAN Infinite® M200 series reader (Morrisville, NC; Ex/Em: 535/587 nm).

Data analysis

Numerical results are presented as mean ± S.E.M.. Sets of numerical data obtained via immunoblot densitometry, cytofluorometric intensities, cholesterol determination, DRAQ7 uptake or cell counts were generally compared by ANOVA followed by Dunnett's test to compare experimental groups with a common control value. Student's t test was used to compare the effect of a single pharmacological intervention on cells otherwise similarly treated. Linear regression presentation and the Pearson's r correlation coefficient were also used to correlate the antiproliferative potency of drugs to other parameters. All computations were performed using the InStat 3.05 computer program, GraphPad Software (San Diego, CA).

Results

Proliferation of cells as modified by s-Et_3N drugs

Four human cellular models were tested for the antiproliferative effects of a series of 6 tertiary amines: the U937 monocytic leukemia cell line, M21 melanoma cells, immortalized HEK 293a cells and primary HUVECs, a non-transformed model of possible relevance for tumoral angiogenesis. 50,000 cells were plated in petri dishes at time zero; drugs were introduced at time 24-hrs and the cells were detached (except for the non-adherent U937 cells) and counted at time 72-hrs (average control counts given in Fig. 1 legend). All 6 tested drug profoundly depressed proliferation in a concentration-dependent manner and with orders of potency that were similar from one cell type to the other. Quinacrine was the most potent proliferation inhibitor, generally followed by amiodarone, chloroquine = hydroxychloroquine, lidocaine and procainamide (Fig. 1). The IC_{50} values recorded for each drug spanned a large concentration range, from approximately 1 μM for quinacrine to 3 mM for procainamide, and these values were roughly inversely correlated with the drug lipophilicity, expressed as logP (Fig. 2).

The proportions of cells in the various phases of the cell cycle was tested in U937 cells (p53-null) and primary HUVECs in response to 48 hr-treatments with a subset of 3 s-Et_3N drugs that span the lipophilicity scale (cytofluorometric assessment of Hoechst 33342 staining, Figs. 3, 4). No consistent effects were observed for cytostatic concentrations of the drugs; some changes may be related to cytotoxic levels of specific drugs, as assessed by high sub-G_1 distributions (particularly for 5 mM procainamide in

U937 cells). Simultaneous determination of the green fluorescence in the same cells evidenced the concentration-dependent accumulation of quinacrine, the only fluorescent s-Et_3N in this portion of the spectrum (Figs. 3, 4). To verify whether a G_0G_1 checkpoint arrest was triggered in s-Et_3N-treated cells, the expression and phosphorylation status of pRB was tested using the same drug sample (48 hr-treatments in in U937 cells or HUVECs, Suppl. Fig. 2, 3). Cationic drug did not consistently promote the dephosphorylation of pRB in HUVECs or U937 cells. Altogether, results support that s-Et_3N induce a desinchronized mitotic arrest.

Autophagy in s-Et_3N-treated U937 cells

Vacuolar cells that have concentrated various amines exhibit an inhibition of the macroautophagic flux (Marceau et al. 1992). One of the two cell lines derived from clinical oncology cases, the U937 cells, was examined for autophagic accumulation during a 6-hr treatment, as assessed with the accumulation of the autophagic effector LC3 II (Fig. 5). The effect of a strong inhibitor of autophagic resolution, the V-ATPase proton pump inhibitor bafilomycin A1, was also recorded in these experiments. It was constantly observed that LC3 II in the total cell extract increased in response to each of the 6 s-Et_3N drugs in a concentration-dependent manner (the exception being amiodarone at 25 μM, an overtly cytotoxic level as will be shown below). The concentration values that produced a threshold LC3 II accumulation (arbitrary intensity of 50) after the short 6 hr-treatment strongly predicted the drug concentration that reduced by 50% the proliferation

of U937 cells (Fig. 6A, correlation of each set of the log(concentration) values: r = 0.94, P<0.01). Procainamide and lidocaine, tested in the same concentration ranges as applied in these experiments, as well as bafilomycin A1 also increased the content of p62/SQSTM1 in U937 cells treated for 6 hrs (data not shown). The analysis presented in Fig. 6B shows that, for each of the 6 s-Et_3N drugs, accumulation of LC3 II (6-hr treatment) is inversely correlated to the final U937 cell counts in the proliferation assay, in a manner largely independent of drug concentration.

Later responses to s-Et_3N drugs in the U937 cells

U937 cells were submitted to additional analyses to characterize events developing later during treatments with cationic drugs. These tests were applied to a large quantity of cells (10^6) treated for 24-48 hrs with drugs concentrations that inhibited cell proliferation by a proportion of one to two thirds to detect typical phenotypes that may be predictive of the anti-tumor action.

More than 90% U937cells excluded the cell impermeant DNA stain DRAQ7 in a viability test based on cytofluorometric analysis (Fig. 7). Actinomycin D treatment (400 nM, 24 hrs) decreased the viability by two-thirds after 24 hrs and by ~80% after 48 hrs of treatment. By contrast, the s-Et_3N drugs were surprisingly well tolerated, with defined concentration(s) of each that were antiproliferative but not cytotoxic. Viability at either time point significantly decreased in cells treated only with 25 μM amiodarone, 100 μM of chloroquine or hydroxychloroquine and 5 mM of lidocaine or procainamide.

An assessment of drug-induced apoptosis was based on the cleavage of PARP1, a late reaction mediated by caspase-3 (Nicholson et al., 1995). In most control cell batches, there was a small proportion of cleaved PARP1 (Fig. 8). 24 hr-treatments with the s-Et_3N drugs generally failed to significantly increase this proportion (except for 25 μM amiodarone and 5 mM lidocaine). Actinomycin D treatment was a positive control, leading to almost complete PARP1 cleavage.

Reversal of the antiproliferative effect of amines by cholesterol ablation

β-cyclodextrin co-treatment is reported to abate the antiproliferative effect of the primary amine leelamine (Kuzu et al., 2014). In experiments reported in Fig. 9, the proliferation assay for U937 cells was modified: 50,000 cells were plated in petri dishes at time zero along with s-Et_3N drugs, with or without β-cyclodextrin co-treatment (1 mM). Cells were counted after 48 hrs of incubation. In this assay, β-cyclodextrin given alone did not alter the ~8-fold proliferation of the cells and did not prevent the complete cell loss induced by actinomycin D (400 nM, a positive control for cytotoxicity). However, β-cyclodextrin co-treatment partially reversed the antiproliferative effect of all 6 substituted triethylamines at amines concentrations eliciting intense effects (generally when the cells counts were below the boxed zone, Fig. 9).

343 Statins inhibit the synthesis of cholesterol at the level of 3-hydroxy-3-methylglutaryl-
344 CoA reductase; the product of the latter enzyme is mevalonic acid. Micromolar
345 concentration levels of lovastatin reportedly inhibit the proliferation of U937 cells (Burke
346 and Kukoly, 2008). In the 48-hr proliferation assay, we used a lower concentration (100
347 nM) that was slightly but significantly antiproliferative (Fig. 10). Lovastatin co-treatment
348 partially but significantly reversed the antiproliferative effect of all s-Et_3N drugs at all
349 tested concentrations, but not that of actinomycin D. The maximal proliferation under
350 lovastatin cotreatment was equivalent to the level observed in cells treated with the statin
351 alone (lower edge of the boxed zone, Fig. 10).

352

353 Some of the effects of statins on cells relate to the inhibition of protein prenylation,
354 mediated by a downstream metabolite of mevalonate, geranylgeranyl-pyrophosphate
355 (GGPP). It has been previously reported that GGPP supplementation (10 μM) of culture
356 medium replenishes cellular pools of isoprenoids (Mohamed et al., 2012). However,
357 GGPP co-treatment had no significant effect on the antiproliferative effect of s-Et_3N
358 compounds (Suppl. Fig. 4).

359

360 *Quinacrine transport in U937 cells*

361 The s-Et_3N drug that possesses enough intrinsic fluorescence for cytofluorometric
362 determination in U937 cells is quinacrine (Suppl. Fig. 5). It was verified that quinacrine
363 concentration by U937 cells is rapid (important in 60 min) and ultimately dependent on
364 V-ATPase acidification of the vacuolar compartment: bafilomycin A1 co-treatment

abrogated the acute cellular uptake of quinacrine in these cells (cytofluorometric or microscopic assays, Suppl. Fig. 5A, B).

To exclude that the gain of proliferative function induced by β-cyclodextrin (Fig. 9) or lovastatin (Fig. 10) might stem from the binding of the s-Et_3N drugs to the oligosaccharide or some other non-specific inhibition of cellular drug uptake, a 48-hr incubation of cells with a low concentration of quinacrine (1 μM, a level that has only modest effect on proliferation) was tested with or without the co-treatments (Suppl. Fig. 6). Cytofluorometric determination of U937 cell fluorescence was not significantly affected by either β-cyclodextrin or lovastatin cotreatment. Those also failed to consistently modify LC3 II accumulation induced by selected cytostatic concentrations of s-Et_3N drugs (48 hr-cotreatments, immunoblots, Suppl. Fig. 7).

Ancillary experiments

The expression of specific proteins was tested in the 4 cellular models used for proliferation studies (immunoblots, Suppl. Fig. 8). U937 cells expressed no p53, consistent with the deletion of both copies of the corresponding gene in its genome (Shiohara et al., 1994); these cells expressed the highest quantity of the LAMP1 protein, possibly indicating a large lysosomal/late endosome compartment. M21 cells, HEK 293a cells and HUVECs expressed variable baseline levels of p62/SQSTM1, LC3, p53 and LAMP1 (Suppl. Fig. 8). The basal concentration of autophagy markers LC3 II and p62/SQSTM1 was comparatively high in M21 melanoma cells.

In U937 cells treated for 48 hrs with β-cyclodextrin or lovastatin, total or free cholesterol was not changed vs. amounts measured in control cells (Suppl. Fig. 9A). However, hydroxychloroquine, one of two tested s-Et_3N drugs at a cytostatic concentration (50 μM), increased total and free cholesterol over 48 hrs; procainamide (2.5 mM) was inactive in this respect (Suppl. Fig. 9B).

A form of vacuolar trafficking was evaluated by the receptor-mediated endosomal uptake of AlexaFluor-594-labeled transferrin (Suppl. Fig. 10). At antiproliferative concentration levels, the s-Et_3N drugs, applied to cells for 24 hrs, generally depressed the subsequent uptake of transferrin, with the notable exception of amiodarone that somewhat increased it at 5-10 μM, but decreased it at 25 μM. Along with the cytofluorometric determination of the cell associated-AlexaFluor-594-labeled transferrin, it was possible to monitor the parallel concentration-dependent uptake of quinacrine (Suppl. Fig. 10, top left). β-Cyclodextrin co-treatment did not modify the effects of s-Et_3Ns on transferrin or quinacrine uptake.

Discussion

Autophagic flux inhibition, usually in the form of oral hydroxychloroquine, is currently considered as an adjuvant to other forms of cancer chemotherapy or radiotherapy, because autophagy is considered as a mechanism of resistance to cytotoxic stress, including acquired resistance to chemotherapeutic agents (Seghal et al., 2015). However, the present results support a widely applicable antiproliferative effect of cationic drugs that interrupt autophagic clearance. The family of 6 s-Et_3N chemicals that we have tested as antiproliferative agents is an arbitrary set of drugs designed to identify molecular determinants of their action, but they are homogeneous if their weak basic properties are considered ($pK_a \geq 8$) and span the lipophilicity scale. They are all highly concentrated in a vacuolar compartment in various cell types in a pseudo-transport process mediated by V-ATPase-mediated ion trapping (Fig. 11, schematic representation). It is remarkable that they share consistent cellular effects (inhibition of the autophagic flux evidenced by LC3 II accumulation, antiproliferative effect relieved by cholesterol ablation) with potencies roughly correlated with their lipophilicity (Fig. 2). High solubility in lipids facilitates the diffusion steps of the molecules towards the vacuolar compartment where they are protonated, sequestered and concentrated (Fig. 11). Amiodarone, the most lipophilic member of the series, is regularly the second or third more potent agent in the various assays, possibly due to its partitioning in all cellular lipids. Evidence for this is provided by a bafilomycin A1-resistant and non-granular component of its cellular uptake monitored by its faint violet fluorescence, which is not the case with quinacrine (Marceau et al., 2012; 2014). A more precise correlation between antiproliferative potency and a biochemical response is provided by the relatively rapid accumulation of the autophagic

effector LC3 II in response to the various s-Et_3Ns (Fig. 5, 6), suggesting that the late response is determined by the early accumulation of cationic drugs in the vacuolar compartment with its consequences stemming from lysosomal incompetence.

The desynchronised cytostatic effect predicted by LC3 II accumulation is the most remarkable effect of s-Et_3Ns in the present study. Overtly cytotoxic/pro-apoptotic effects were recorded for at supra-cytostatic concentrations of most of these drugs, but the mechanism does not need to be uniform. Amiodarone at 25 μM is overtly cytotoxic (Fig. 9) and cells treated with this drug level accordingly exhibits an anomalous decrease of LC3 II content relative to cells treated with tolerated concentrations (Fig. 5). A known toxicity of mitochondrial origin for millimolar lidocaine (Johnson et al., 2004) may explain apoptotic cell death at 5 mM (Fig. 7, 8). Other Et_3Ns are reportedly DNA-binding at certain concentrations: chloroquine (10-500 μM; Allison et al., 1965), quinacrine (Ehsanian et al., 2011; Macfarlane and Manzel, 1998) and procainamide (Thomas and Messner, 1986). However, the s-Et_3N that best supports cell imaging via its intrinsic fluorescence, quinacrine, did not stain nuclei of U937 cells in the presence of bafilomycin A1 (Suppl. Fig. 5), tending to exclude DNA binding as a significant mechanism for its cytostatic action.

In a recent study, the lipophilic cationic drug leelamine induced apoptosis in a tumor cell line; this was parallel to the vacuolar accumulation of free cholesterol and reversed by cholesterol extraction using β-cyclodextrin. We have observed partial inhibition of the

449 antiproliferative effect of the 6 s-Et_2Ns on U937 cells by co-treatment with β-
450 cyclodextrin and extended this approach to a drug that inhibits cholesterol synthesis, a
451 statin. Either intervention applied at an intensity that was not toxic failed to decrease the
452 free or esterified cholesterol over 48 hrs in U937 cells (Suppl. Fig. 9A), consistent with
453 the idea that narrow tolerance exists in these cells for cholesterol depletion (Burke and
454 Kukoly, 2008). Further, at the examined time point, only one of 2 tested s-Et_3N at a
455 cytostatic concentration significantly increased cell cholesterol content (Suppl. Fig. 9B).
456 The anti-cholesterol interventions had no systematic effect on autophagic flux inhibition
457 by the s-Et_3Ns (Suppl. Fig. 7) or on quinacrine uptake (Suppl. Fig. 6). However, β-
458 cyclodextrin may redistribute cholesterol between cell compartments: a derivative is
459 being evaluated to remove cholesterol accumulated in lysosomes in Niemann-Pick type C
460 disease (Santos-Lozano et al., 2015). Further, β-cyclodextrin reverses cholesterol
461 accumulation in atherosclerotic plaques in an animal model (Zimmer et al., 2016). The
462 cytopathology induced by cationic drugs also includes a non-specific depression of
463 vacuolar trafficking affecting both endocytosis and secretion (Marceau et al., 2012), a
464 finding generally reproduced in the present study by the depression of transferrin uptake
465 in U937 cells (Suppl. Fig. 10). However, s-Et_3N-induced depression of transferrin uptake
466 in U937 cells was not affected by β-cyclodextrin co-treatment. Kuzu et al. (2014)
467 observed the inhibition of receptor-induced endocytosis, but were more interested to
468 study the cytotoxic concentration levels of their test cationic drug, leelamine. More work
469 is needed, notably ultrastructural studies of phospholipidosis and autophagosomes, to
470 pinpoint a critical step sensitive to cholesterol redistribution that leads to a
471 desynchronized mitotic arrest in cells that accumulated cationic drugs.

Whether the antiproliferative effect of cationic drugs can be exploited in oncology is of practical interest, whether they are administered in combination or alone. We observed a lack of cell type specificity as well as a graded action that involved a cytostatic effect at lower drug concentrations. On the other hand, all the tested cell types were highly proliferative *in vitro* and, in a cancer therapeutic strategy, toxicity to quiescent tissues may be tolerable. The superiority of quinacrine over chloroquine and hydroxychloroquine is noteworthy; effective quinacrine distribution to a tumor xenograft has recently been observed in mice (Golden et al., 2015). Further, some of our original or confirmatory findings on antiproliferative actions, such as p53 independence (a potential advantage), possible biomarker value of tumoral LC3 II accumulation and antagonism by a statin (a widely used drug class), may be of clinical interest.

Conclusion

The inhibition of autophagic flux is a major predictor of the desynchronized and p53-independent cytostatic effect of cationic drugs, along with the facilitator effect of drug liposolubility.

Competing interests

The authors declare that they have no competing interests.

Funding

Supported by the Natural Sciences and Engineering Research Council of Canada [operating grant to F.M.] and the grant MOP-93773 from the Canadian Institutes of Health Research [operating grant to F.M.].

Acknowledgemnts

We thank Dr. Marc Pouliot for facilitating the access to microscopic equipment, Dr. Alexandre Brunet for operating the cytofluorometry equipment, and Ms. Johanne Bouthillier for technical help.

References

Allison, J.L., O'Brien, R.L., Hahn, F.E., 1965. DNA: reaction with chloroquine. Science 149, 1111-1113.

Bao, W., Strömblad, S., 2004. Integrin αv-mediated inactivation of p53 controls a MEK1-dependent melanoma cell survival pathway in three-dimensional collagen. J. Cell Biol. 167, 745-756.

Bawolak, M.T., Morissette, G., Marceau, F., 2010. Vacuolar ATPase-mediated sequestration of local anesthetics in swollen macroautophagosomes. Can. J. Anesth. 57, 230-239.

Briceno, E., Calderon, A., Sotelo, J., 2007. Institutional experience with chloroquine as an adjuvant to the therapy for glioblastoma multiforme. Surg. Neurol. 67, 388-391.

Burke, L.P., Kukoly, C.A., 2008. Statins induce lethal effects in acute myeloblastic lymphoma cells within 72 hours. Leukemia Lymphoma 49, 322-330.

Ehsanian, R., Van Waes, C., Feller, S.M., 2011. Beyond DNA binding – a review of the potential mechanism mediating quinacrine's therapeutic activities in parasitic infections, inflammation and cancers. Cell Communic. Signaling 9, 13.

Golden, E.B., Cho, H.Y., Hofman. F.M., Louie, S.G., Schonthal, A.H., Chen, T.C., 2015. Quinoline-based antimalarial drugs: a novel class of autophagy inhibitors. Neurosurg. Focus 38. E12.

Johnson, M.E., Uhl, C.B., Spitler, K.H., Wang, H., Gores, G.J., 2004. Mitochondrial injury and caspase activation by the local anesthetic lidocaine. Anesthesiology 101. 1184-1194.

Koumbadinga, G.A., Désormeaux, A., Adam, A., Marceau, F., 2010. Effect of interferon-γ on inflammatory cytokine-induced bradykinin B_1 receptor expression in human vascular cells. Eur. J. Pharmacol. 647, 117-125.

Kuzu, O.F., Gowda, R., Sharma, A., Robertson, G.P., 2014. Leelamine mediates cancer cell death through inhibition of intracellular cholesterol transport. Mol. Cancer Ther. 13, 1690-1703.

Macfarlane, D.E., Manzel, L., 1998. Antagonism of immunostimulatory CpG-oligodeoxynucleotides by quinacrine, chloroquine, and structurally related compounds. J. Immunol. 160, 1122-1131.

Marceau, F., Bawolak, M.T., Lodge, R., Bouthillier, J., Gagné-Henley, A., Gaudreault, R.C., Morissette, G., 2012. Cation trapping by cellular acidic compartments: beyond the concept of lysosomotropic drugs. Toxicol. Appl. Pharmacol. 259, 1-12.

Marceau, F., Roy, C., Bouthillier, J., 2014. Assessment of cation trapping by cellular acidic compartments. Methods Enzymol. 534, 119-131.

McMahon, G.A., Petitclerc, E., Stefansson, S., Smith, E., Wong, M.K.K., Ginsburg, D., Brooks, P.C., Lawrence, D.A., 2001. Plasminogen activator inhibitor-1 regulates tumor growth and angiogenesis. J. Biol. Chem. 276, 33964-33968.

Mohamed, A., Saavedra, L., Di Pardo, A., Sipoine, S., Posse de Chaves, E., 2012. β-Amyloid inhibits protein prenylation and induces cholexterol sequestration by impairing SREBP-2 cleavage. J. Neurosci. 32, 6490-6500.

560 Morissette, G., Germain, L., Marceau, F., 2007. The antiwrinkle effect of topical
561 concentrated 2-dimethylaminoethanol involves a vacuolar cytopathology. Br. J.
562 Dermatol. 156, 433-439.

563

564 Morissette, G., Moreau, E., C.-Gaudreault, R., Marceau, F., 2004. Massive cell
565 vacuolization induced by organic amines such as procainamide. J. Pharmacol. Exp. Ther.
566 310, 395-406.

567

568 Morissette, G., Lodge, R., Marceau, F.. 2008. Intense pseudotransport of a cationic drug
569 mediated by vacuolar ATPase: procainamide-induced autophagic cell vacuolization. Tox.
570 Appl. Pharmacol. 228, 364-377.

571

572 Morissette, G., Moreau, E., C.-Gaudreault, R., Marceau, F., 2005. N-substituted 4-
573 aminobenzamides (procainamide analogs): an assessment of multiple cellular effects
574 concerning ion trapping. Mol. Pharmacol. 68, 1576-1589.

575

576 Nicholson, D.W., Ali, A., Thornberry, N.A., Vaillancourt, J.P., Ding, C.K., Gallant, M.,
577 Gareau, Y., Griffin, P.R., Labelle, M., Lazebnik, Y.A., et al.. 1995. Identification and
578 inhibition of the ICE/CED-3 protease necessary for mammalian apoptosis. Nature 376.
579 37-43.

Nioi, P., Perry, B.K., Wang, E.J., Gu, Y.Z., Snyder, R.D., 2007. In vitro detection of drug-induced phospholipidosis using gene expression and fluorescent phospholipid based methodologies. Toxicol. Sci. 99, 162-173.

Oliveiro, S., Amendola, A., Di Sano, F., Farrace, M.G., Fesus, L., Nemes, Z., Piredda, L., Spinedi, A., Piacentini, M., 1997. Tissue transglutaminase-dependent posttranslational modification of the retinoblastoma gene product in promonocytic cells undergoing apoptosis. Mol. Cell Biol. 17, 6040-6048.

Parks, A., Charest-Morin, X., Boivin-Welch, M., Bouthillier, J., Marceau, F. 2015. Autophagic flux inhibition and lysosomogenesis ensuing cellular capture and retention of the cationic drug quinacrine in murine models. PeerJ 3, e1314.

Roy, C., Gagné, V., Fernandes, M.J.G., Marceau, F., 2013. High affinity capture and concentration of quinacrine in polymormonuclear neutrophils via vacuolar ATPase-mediated ion trapping: comparison with other peripheral blood leukocytes and implications for the distribution of cationic drugs. Tox. Appl. Pharmacol. 270, 77-86.

599 Santos-Lozano, A., Villamandos García, D., Sanchis-Gomar, F., Fiuza-Luces, C., Pareja-
600 Galeano, H., Garatachea, N., Nogales Gadea, G., Lucia, A., 2015, Niemann-Pick disease
601 treatment: a systematic review of clinical trials. Ann. Transl. Med. 3, 360.

602

603 Sawada, H., Takami, K., Asahi, S.A., 2005. Toxicogenomic approach to drug-induced
604 phospholipidosis: analysis of its induction mechanism and establishment of a novel in
605 vitro screening system. Toxicol. Sci. 83, 282–292.

606

607 Sehgal, A.R., Konig, H., Johnson, D.E., Tang, D., Amaravaldi, R.K., Boyiadzis, M.,
608 Lotze, M.T., 2015. You eat what you are: autophagy inhibition as a therapeutic strategy
609 in leukemia. Leukemia 29, 517-525.

610

611 Shiohara, M., el-Deiry, W.S., Wada, M., Nakamaki, T., Takeuchi, S., Yang, R., Chen,
612 D.L., Vogelstein, B., Koeffler, HéP., 1994. Absence of WAF1 mutations in a variety of
613 human malignancies. Blood 84, 3781–3784.

614

615 Thoburn, A., Thamm, D.H., Gustafson, D.L., 2014. Autophagy and cancer therapy. Mol.
616 Pharmacol. 85, 830-838.

617

618 Thomas, T.J., Messner, R.P., 1986. Effects of lupus-inducing drugs on the B to Z
619 transition of synthetic DNA. Arthritis Rheum. 29, 638-645.

620

621 Zhang, X., Liu, X., Shang, H., Xu, Y., Qian, M., 2011. Monocyte chemoattractant
622 protein-1 induces endothelial cell apoptosis in vitro through a p53-dependent
623 mitochondrial pathway. Acta Biochim. Biophys. Sin. (Shanghai) 43, 787-795.

624

625 Zimmer, S., Grebe, A., Bakke, S.S., Bode, N., Halvorsen, B., Ulas, T., Skjelland, M., De
626 Nardo, D., Labzin, L.I., Kerksiek, A., Hempel, C., Heneka, M.T., Hawxhurst, V.,
627 Fitzgerald, M.L., Trebicka, J., Björkhem, I., Gustafsson, J.Å., Westerterp, M., Tall, A.R.,
628 Wright, S.D., Espevik, T., Schultze, J.L., Nickenig, G., Lütjohann, D., Latz, E., 2016,
629 Cyclodextrin promotes atherosclerosis regression via macrophage reprogramming. Sci.
630 Transl. Med. 8, 333ra50.

631 **Figure legends**

632

633 Fig. 1. Effect of substituted trimethylamine (s-Et_3N) drugs on the proliferation of 4
634 cultured cell types. 50,000 cells were seeded in petri dishes 72 hrs before counts in the
635 serum-containing medium appropriate for each cell type (drugs present for the last 48
636 hrs). Cell counts are normalized as a percent of the control values recorded in each day of
637 experiments. The absolute control counts at 72 hrs were 946,592 ± 51,976 (n = 38) for
638 U937 cells, 484,597 ± 24,501 (n = 36) for M21 cells, 308,315 ± 9,089 (n = 36) for
639 HUVECs and 528,015 ± 22,496 (n = 34) for HEK 293a cells.

640

641 Fig. 2. Possible correlation between the antiproliferative IC_{50} values of 6 s-Et_3N drugs
642 derived from 4 cell types and their lipophilicity, expressed as logP (logP values are from
643 http://chembank.broadinstitute.org/). The x-axis coordinates of the points correspond to a
644 specific lipophilicity associated with the drug named below. The y-axis coordinates are
645 derived from Fig. 1 data. The 4 represented cell types and the linear regression applicable
646 to each cell type are indicated by the symbol and line colors.

647

648 Fig. 3. Cell cycle analysis based on cytofluorometric determination of Hoechst 33342 in
649 U937 cells treated for 48 hrs with selected s-Et_3Ns. Top left: histograms representing the
650 proportion of the cells in each cell cycle phase in duplicated experiments. Bottom: sample
651 cytofluorometric recordings corresponding to experimental conditions indicated by lower

652 case letters. Top right: green fluorescence intensity simultaneously recorded in the same
653 cells.

654

655 Fig. 4. Cell cycle analysis based on cytofluorometric determination of Hoechst 33342 in
656 primary HUVECs treated for 48 hrs with selected s-Et_3Ns. Triplicate determinations in
657 cell lines established from separate donors. Presentation as in Fig. 3.

658

659 Fig. 5. Immunoblot of LC3 in extracts of U937 cells treated with s-Et_3Ns. The cells were
660 submitted to the indicated drug treatment for 6 hrs. Top: representative immunoblots,
661 showing the concentration-dependent decrease of LC3 I and accumulation of LC3 II.
662 Equal loading of tracks, documented with the immunoblots of β-actin, is shown for
663 amiodarone-treated cells. Bottom: densitometric values of LC3 II in replicated
664 experiments (n = 3-4).

665

666 Fig. 6. Prediction of the antiproliferative effects of s-Et_3N drugs by early LC3 II
667 accumulation. A. Correlation between the potencies of s-Et_3N drugs in the proliferation
668 assay (48-hr treatments, Fig. 1, top left) and in the LC3 II accumulation (6-hr treatment,
669 Fig. 5) in U937 cells. B. Correlation between LC3 II and cell counts for individual s-
670 Et_3Ns. The LC3 II intensity value of 100 or higher were excluded, as well as the value
671 from cells treated with the cytotoxic concentration of amiodarone (25 μM). Linear

672 regressions generally are of the same color as the experimental points of each drug
673 (yellow: procainamide; dashed black: chloroquine). See Results for further description.

674

675 Fig. 7. Viability of U937 cells as estimated by cytofluorometric determination of DRAQ7
676 staining. Cells were treated as indicated for 24 or 48 hrs with the indicated drug. Results
677 are expressed as the proportion of cells excluding the DNA stain. ANOVA indicated that
678 the set of values is heterogeneous (24 hr-treatments: $P<10^{-4}$; 48 hr-treatments: $P<10^{-4}$).
679 The effect of individual treatments was tested using Dunnett's test (* $P<0.05$; ** $P<0.01$
680 vs. control values for each time point). Sample cell distributions (24 hr-treatments) are
681 shown as insets.

682

683 Fig. 8. PARP1 cleavage induced by 24 hr-drug treatments in U937 cells. A. Sample
684 immunoblots. B. Proportion of cleaved PARP1 derived from densitometry in replicated
685 experiments. ANOVA indicated that the set of values is heterogeneous ($P<10^{-4}$). The
686 effect of individual treatments was tested using Dunnett's test (* $P<0.01$ vs. control
687 value).

688

689 Fig. 9. Partial reversal of the antiproliferative effects of s-Et_3Ns by co-treatment with β-
690 cyclodextrin (1 mM) in U937 cells. 50,000 cells were seeded in petri dishes containing
691 serum-supplemented medium 48 hrs before counts and all drugs were present during the
692 whole incubation period. Actinomycin D is a positive control. Values are means ± s.e.m.

693 of at least 6 determinations. The effect of β-cyclodextrin co-treatment at each dose level
694 of each drug: * P<0.05; ** P<0.01; *** P< 0.001 (Student's t test).

695

696 Fig. 10. Partial reversal of the antiproliferative effects of s-Et_3Ns by co-treatment with
697 lovastatin (100 nM) in U937 cells. 50,000 cells were seeded in petri dishes containing
698 serum-supplemented medium 48 hrs before counts and all drugs were present during the
699 whole incubation period. Actinomycin D is a positive control. Values are means ± s.e.m.
700 of at least 4 determinations. The effect of lovastatin co-treatment at each dose level of
701 each drug: * P<0.05; ** P<0.01; *** P< 0.001 (Student's t test).

702

703 Fig. 11. Schematic representation of cellular responses to s-Et_3Ns and mode of action of
704 selected experimental interventions on the system.

705

June 3, 2016

Editor-in-Chief
Toxicology and Applied Pharmacology

RE: TAAP-D-16-00294

Dear Sir,

Thank you for reviewing our manuscript entitled " Lysosomotropic cationic drugs induce cytostatic and cytotoxic effects relieved by cholesterol ablation: analysis of a substituted triethylamine series."

We would like to submit a revised version of the work that incorporates changes and clarifications requested by Reviewers. The changes are highlighted in yellow. I will also upload a detailed letter that includes replies to Reviewers and changes made to the manuscript.

We thank you in advance for your consideration.

Sincerely yours,

François Marceau, M.D., Ph.D.
Corresponding author
Professor
Axe Maladies Infectieuses et Immunitaires
CHU de Québec-Université Laval
Québec QC
Canada G1V 4G2

Tel. (418) 525-4444 ext. 46155
FAX: (418) 654-2765
E-mail: francois.marceau@crchul.ulaval.ca

Graphical Abstract

graphical abstract

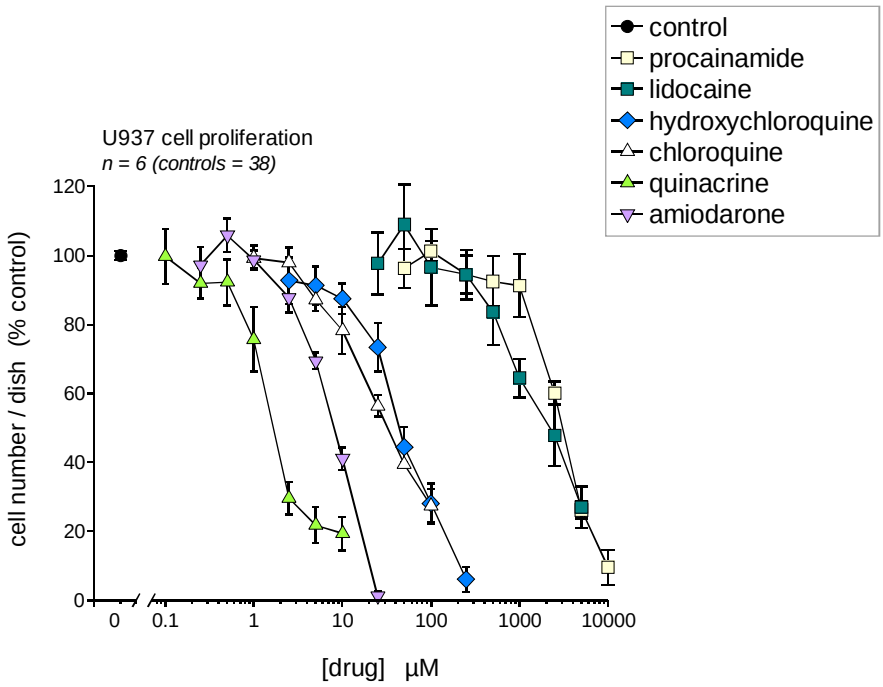

Figure 1

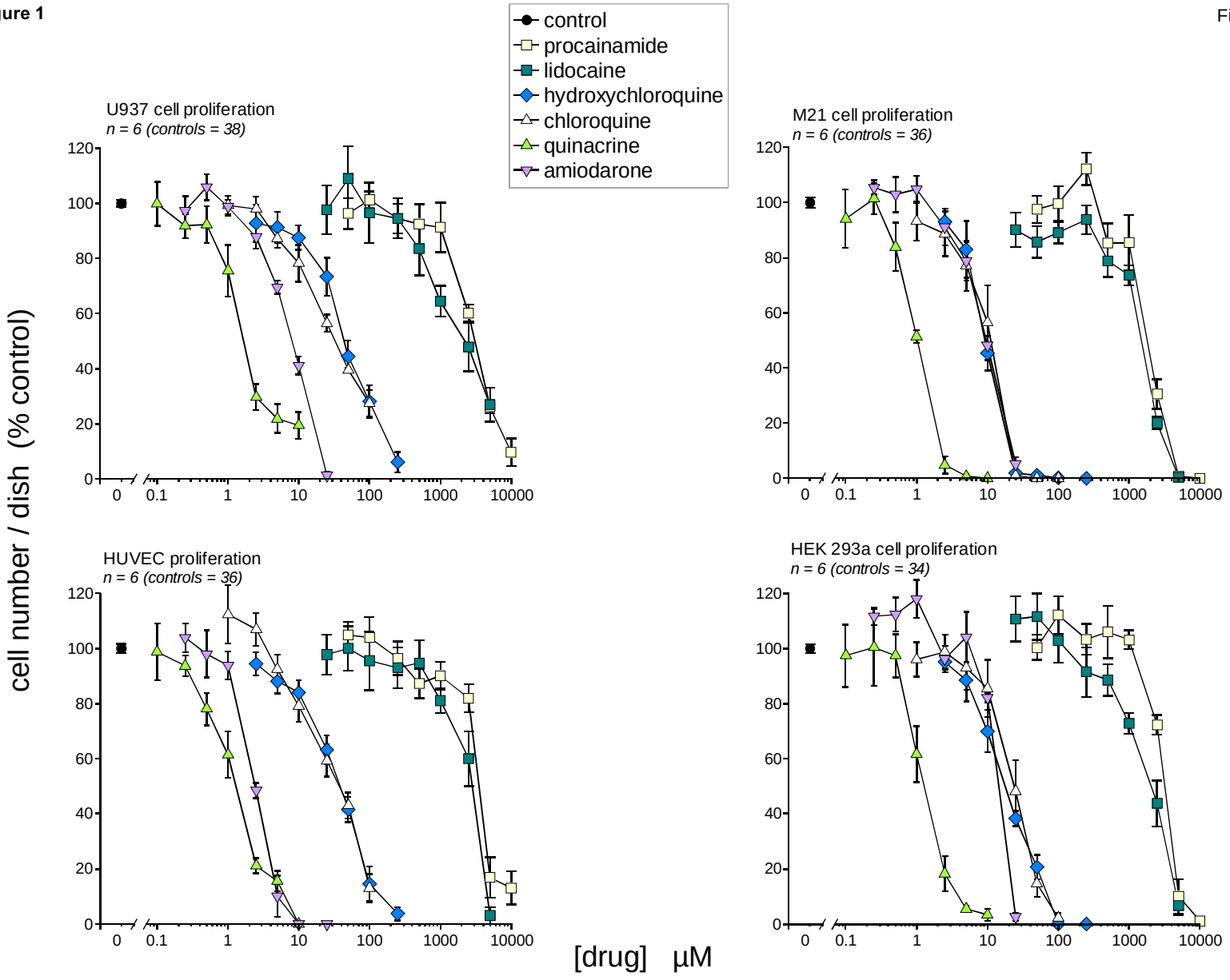
control
procainamide
lidocaine
hydroxychloroquine
chloroquine
quinacrine
amiodarone
U937 cell proliferation
n = 6 (controls = 38)
M21 cell proliferation
n = 6 (controls = 36)
HUVEC proliferation
n = 6 (controls = 36)
HEK 293a cell proliferation
n = 6 (controls = 34)
cell number / dish (% control)
[drug] µM
0
20
40
60
80
100
120
0
0.1
1
10
100
1000
10000

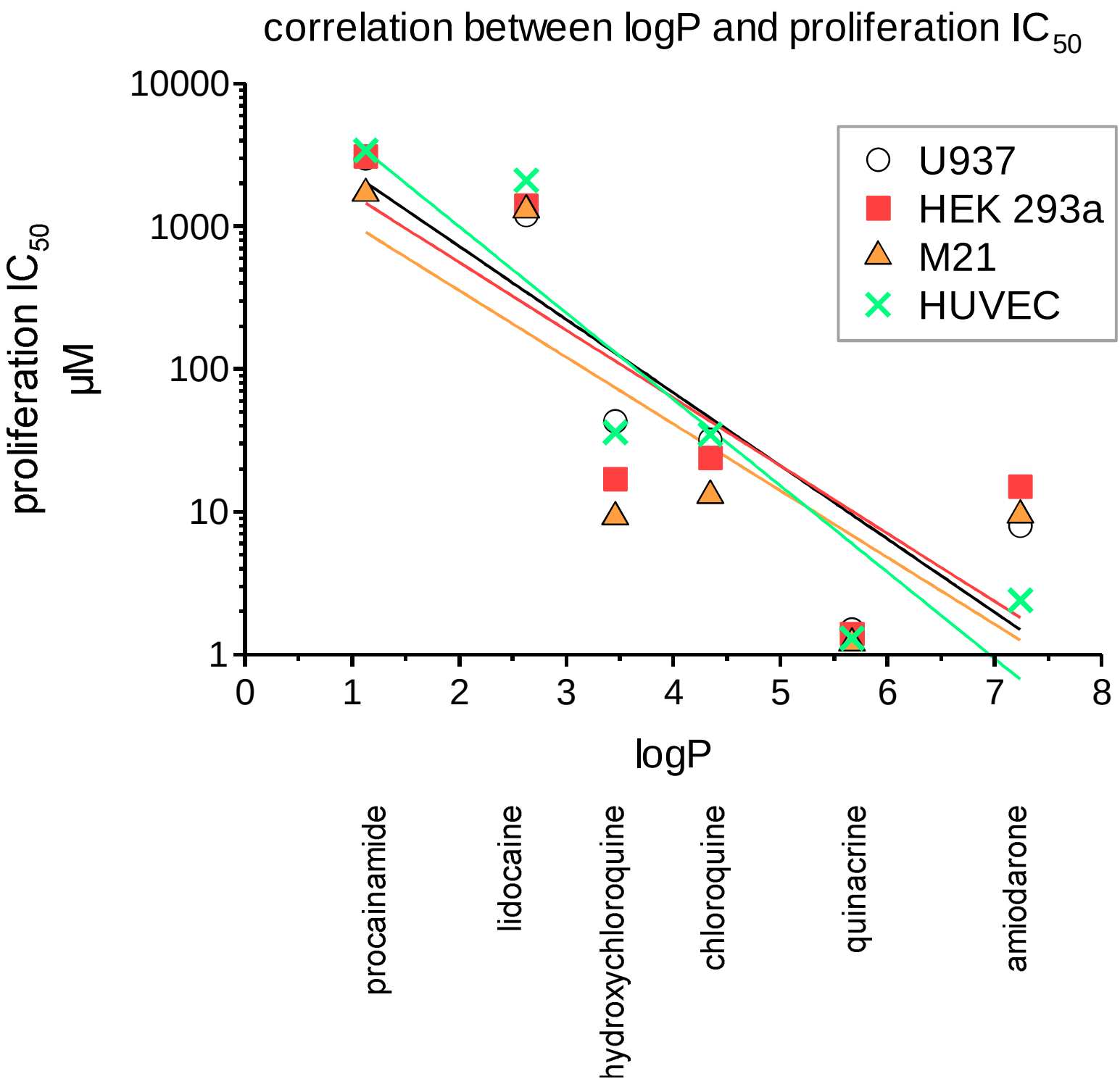
correlation between logP and proliferation IC50
proliferation IC50
µM
10000
1000
100
10
1
0
1
2
3
4
5
6
7
8
logP
U937
HEK 293a
M21
HUVEC
procainamide
lidocaine
hydroxychloroquine
chloroquine
quinacrine
amiodarone

Figure 3

Fig. 3

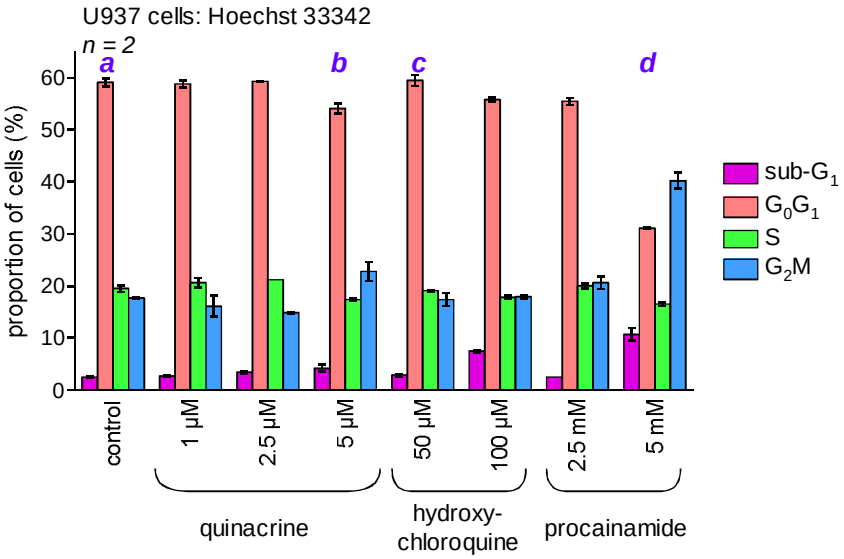

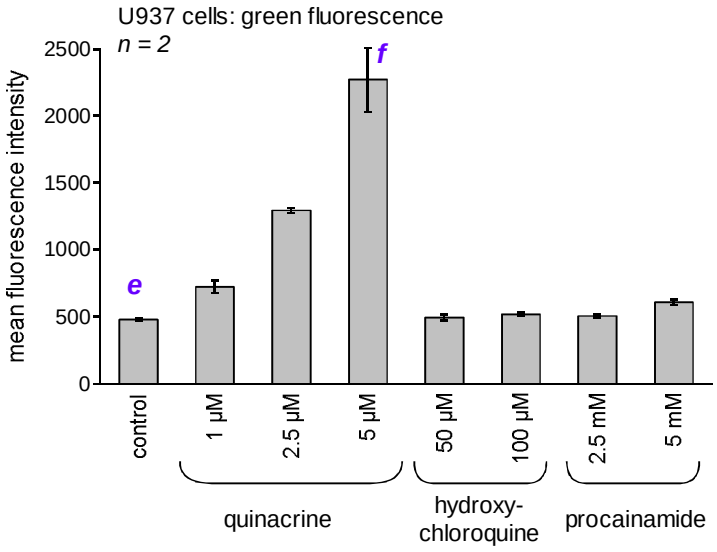

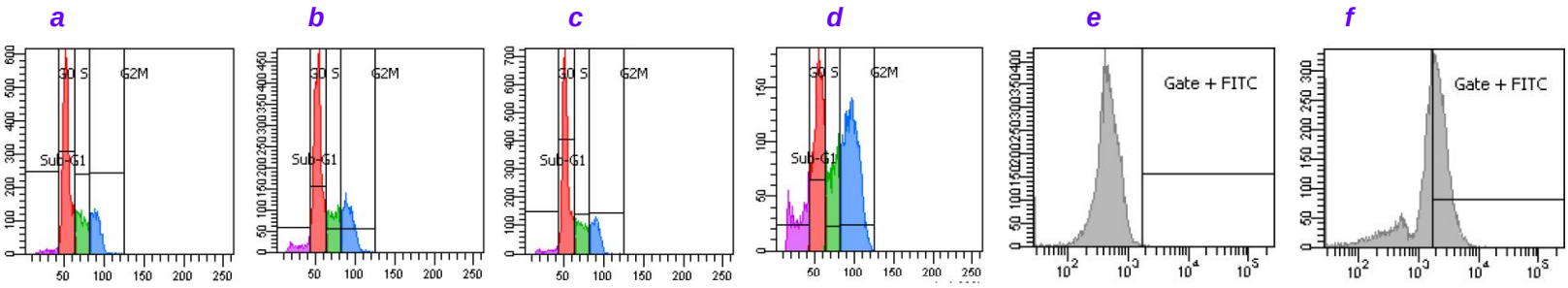

Figure 4

Fig. 4

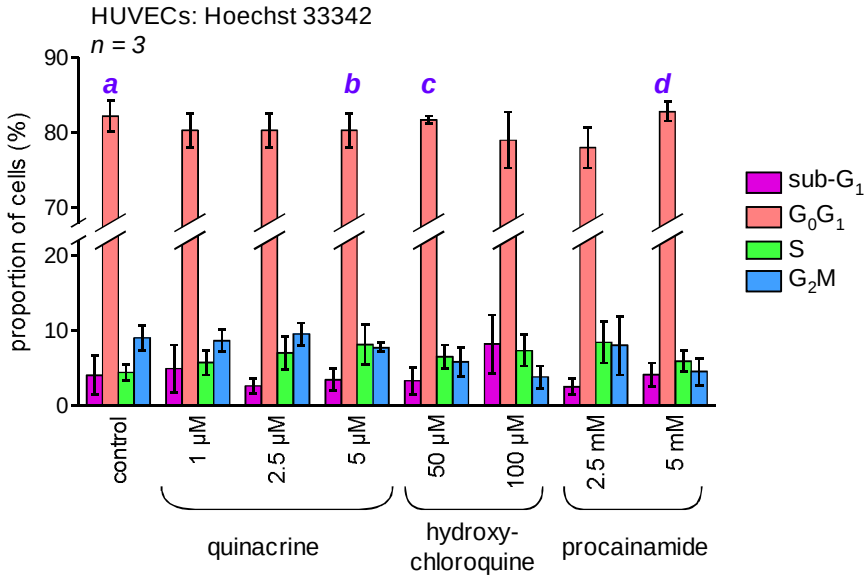

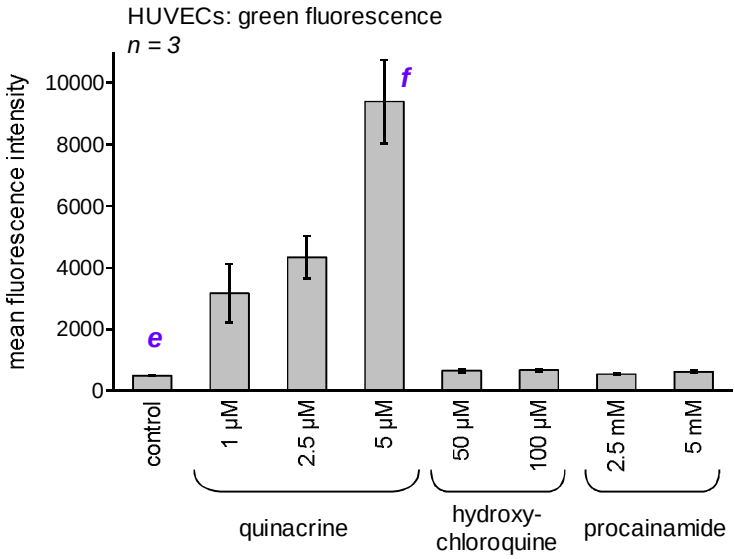

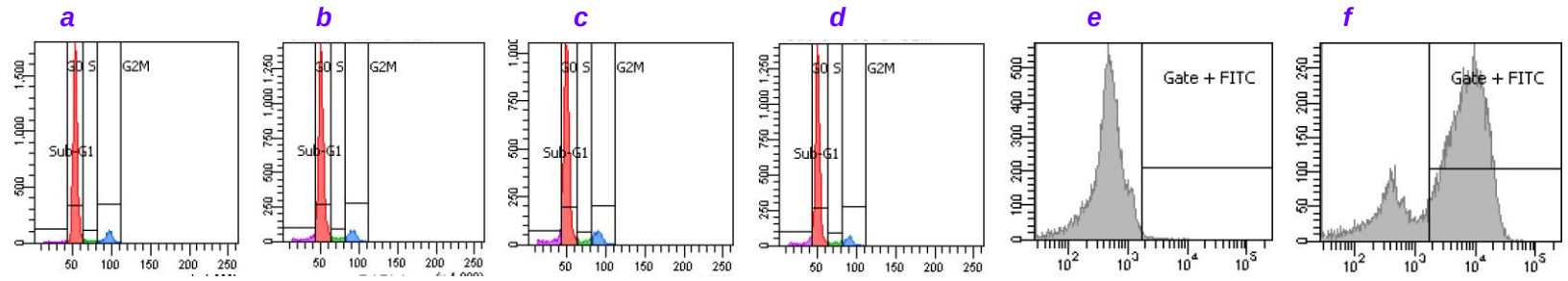

U937 cells
6-hr treatments

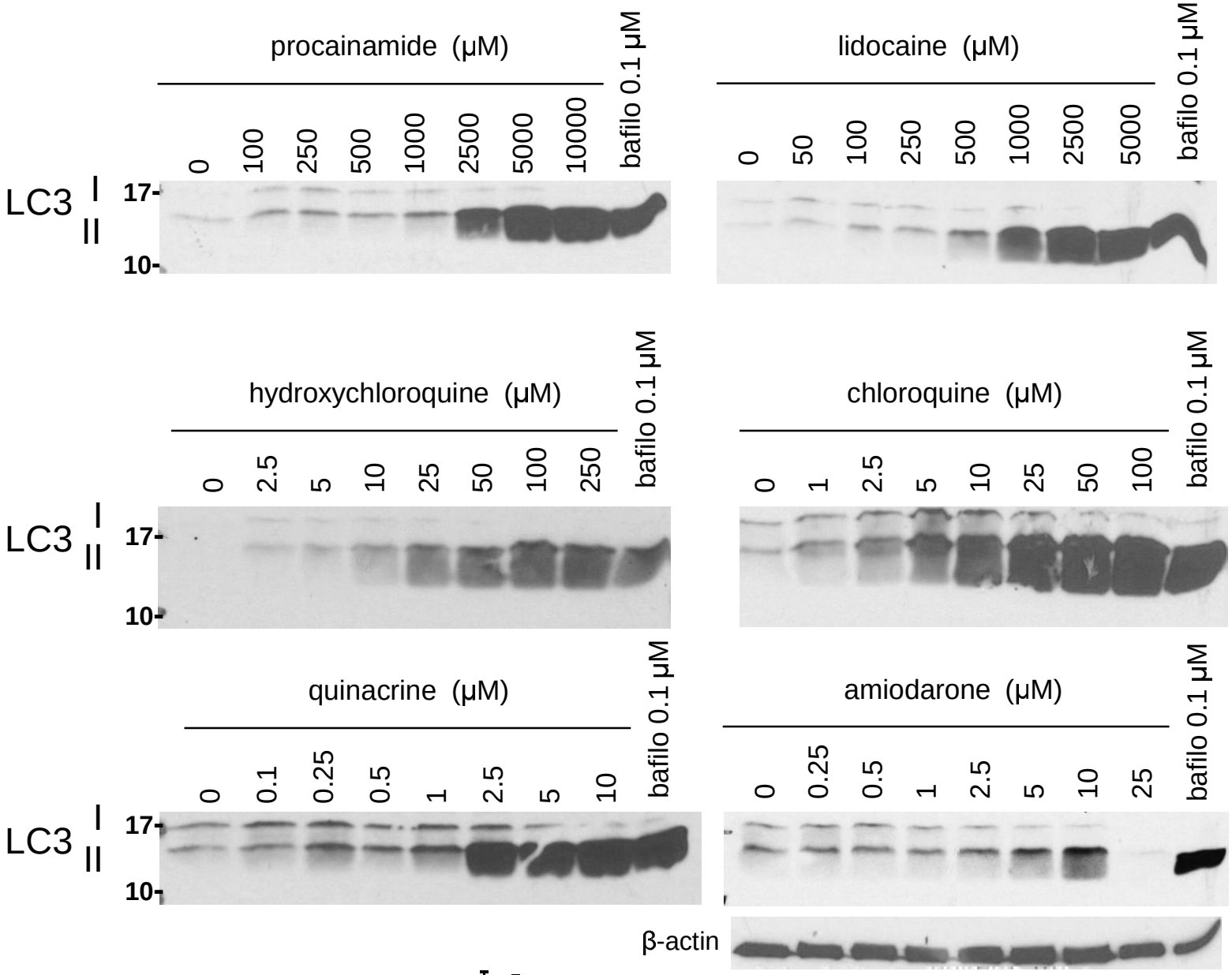

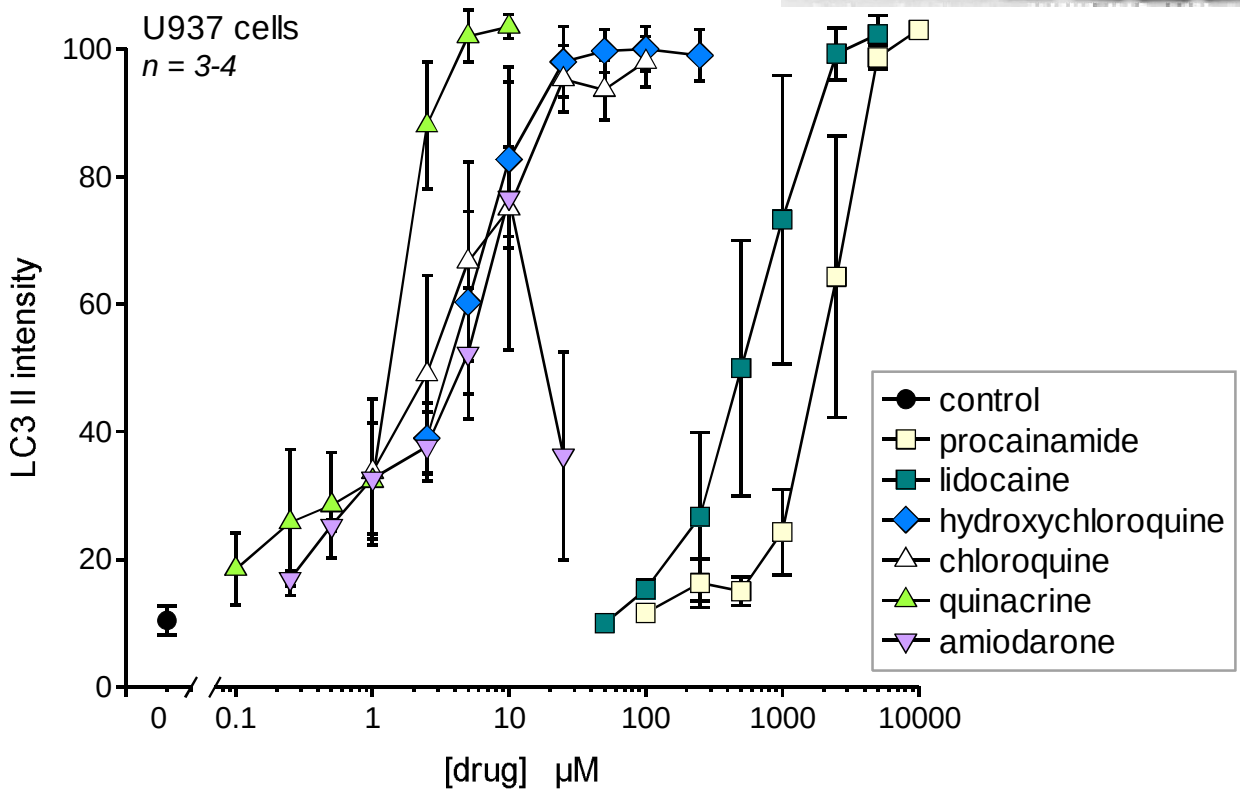

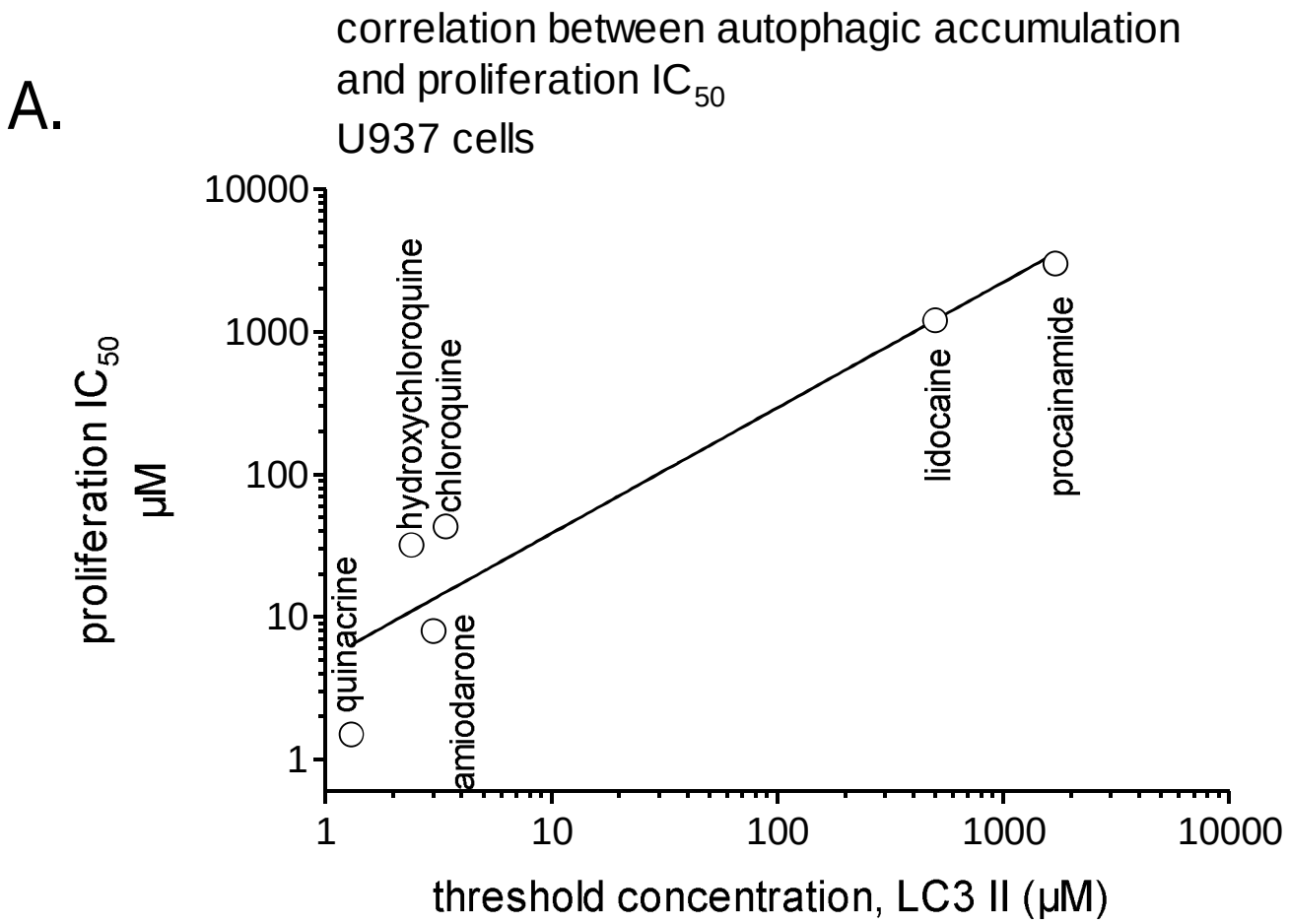
A.
correlation between autophagic accumulation
and proliferation IC50
U937 cells
proliferation IC50
µM
10000
1000
100
10
1
quinacrine
hydroxychloroquine
chloroquine
amiodarone
lidocaine
procainamide
1
10
100
1000
10000
threshold concentration, LC3 II (µM)

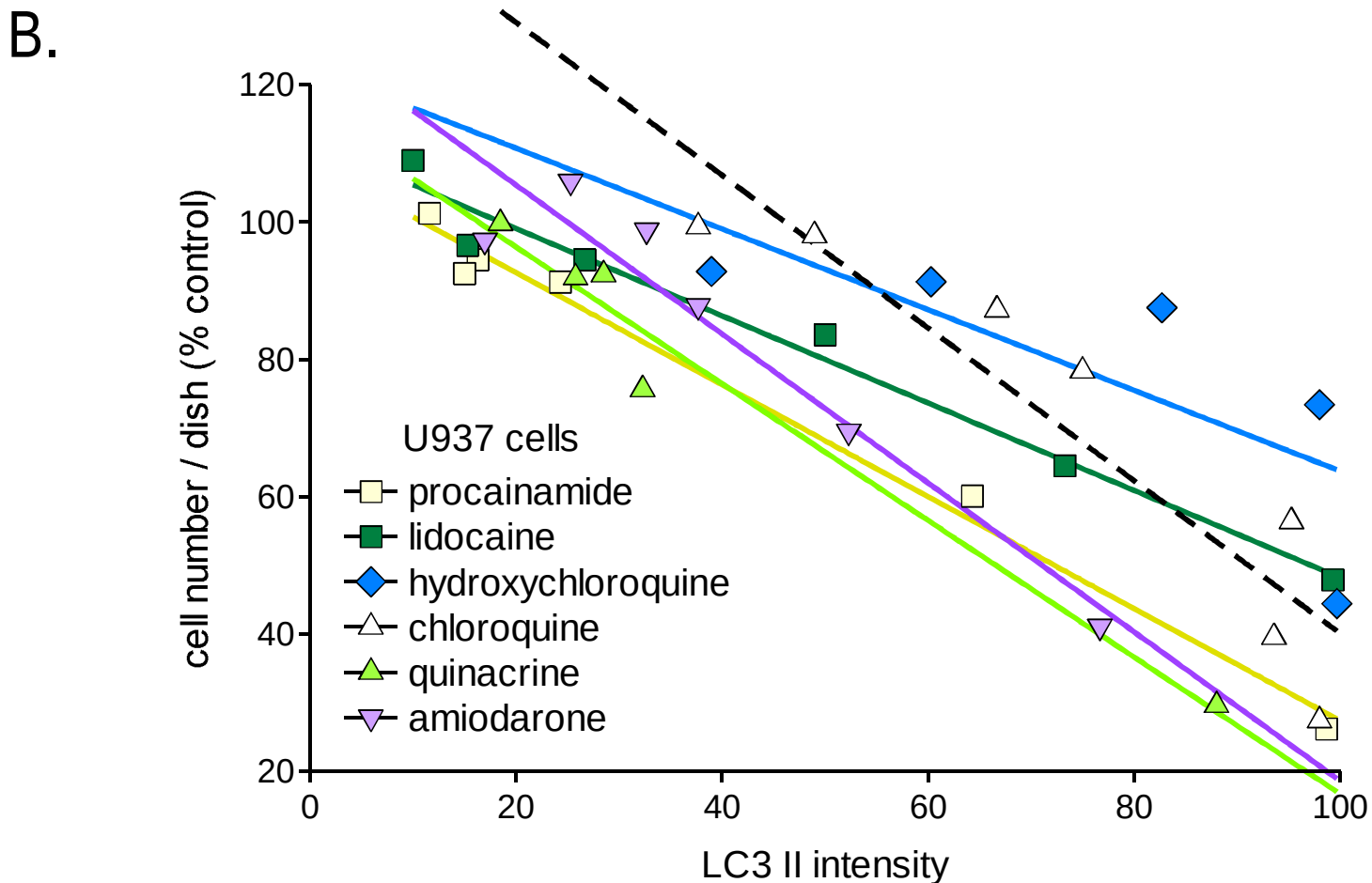
B.
cell number / dish (% control)
120
100
80
60
40
20
U937 cells
procainamide
lidocaine
hydroxychloroquine
chloroquine
quinacrine
amiodarone
0
20
40
60
80
100
LC3 II intensity

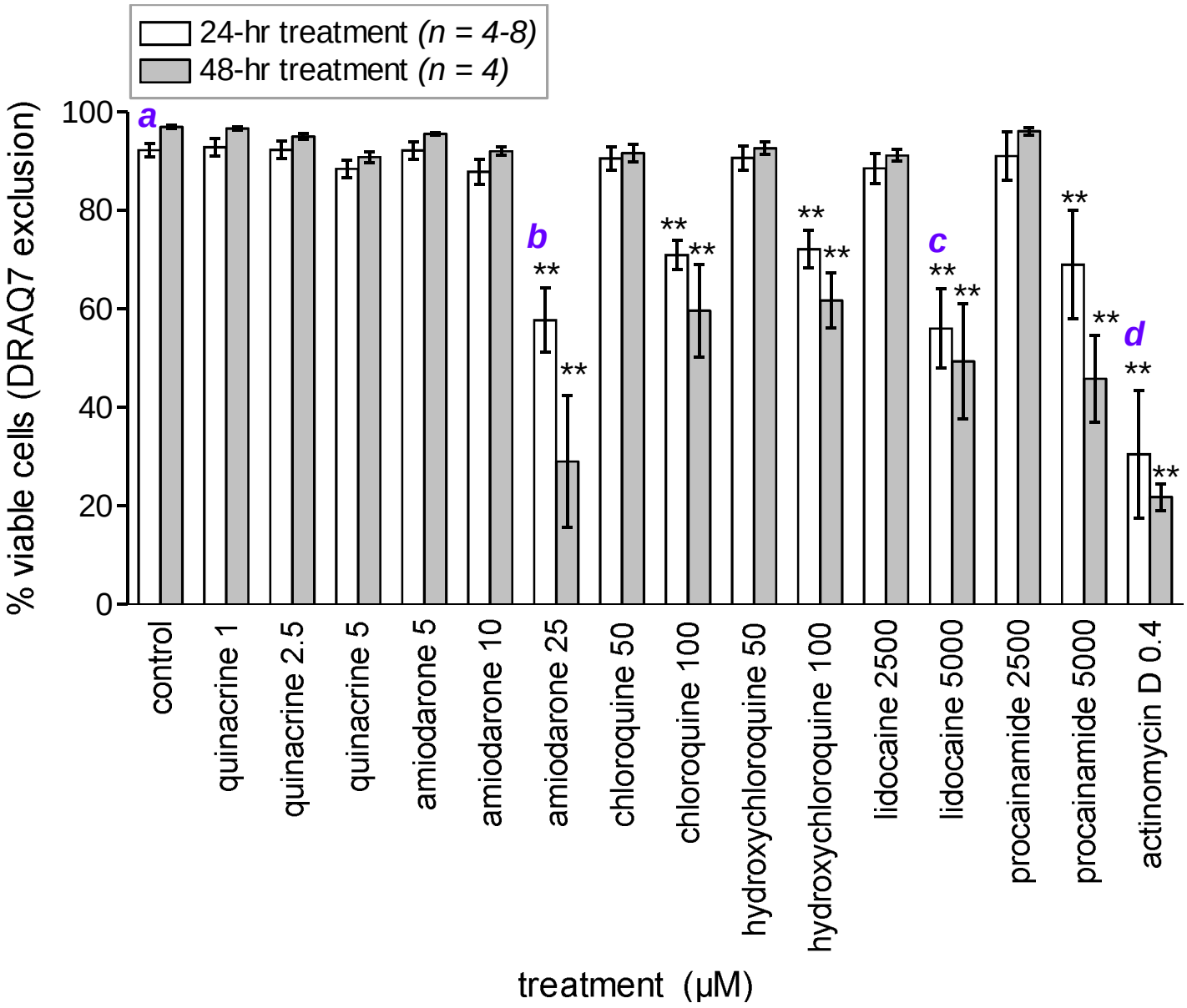
24-hr treatment (n = 4-8)
48-hr treatment (n = 4)
% viable cells (DRAQ7 exclusion)
100
80
60
40
20
0
a
b
c
d
**
control
quinacrine 1
quinacrine 2.5
quinacrine 5
amiodarone 5
amiodarone 10
amiodarone 25
chloroquine 50
chloroquine 100
hydroxychloroquine 50
hydroxychloroquine 100
lidocaine 2500
lidocaine 5000
procainamide 2500
procainamide 5000
actinomycin D 0.4
treatment (μM)

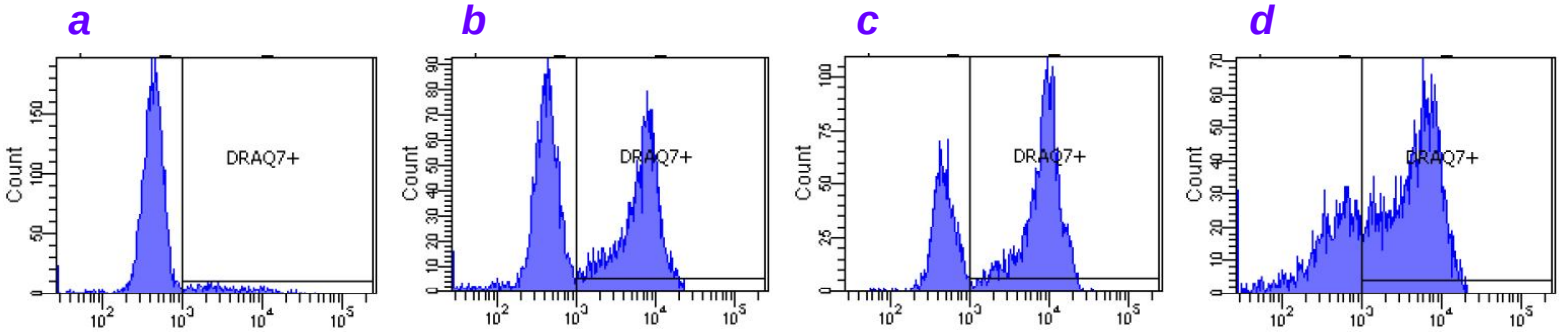
a
b
c
d
Count
DRAQ7+

A.

U937 cells
24 hr-treatments
PARP1

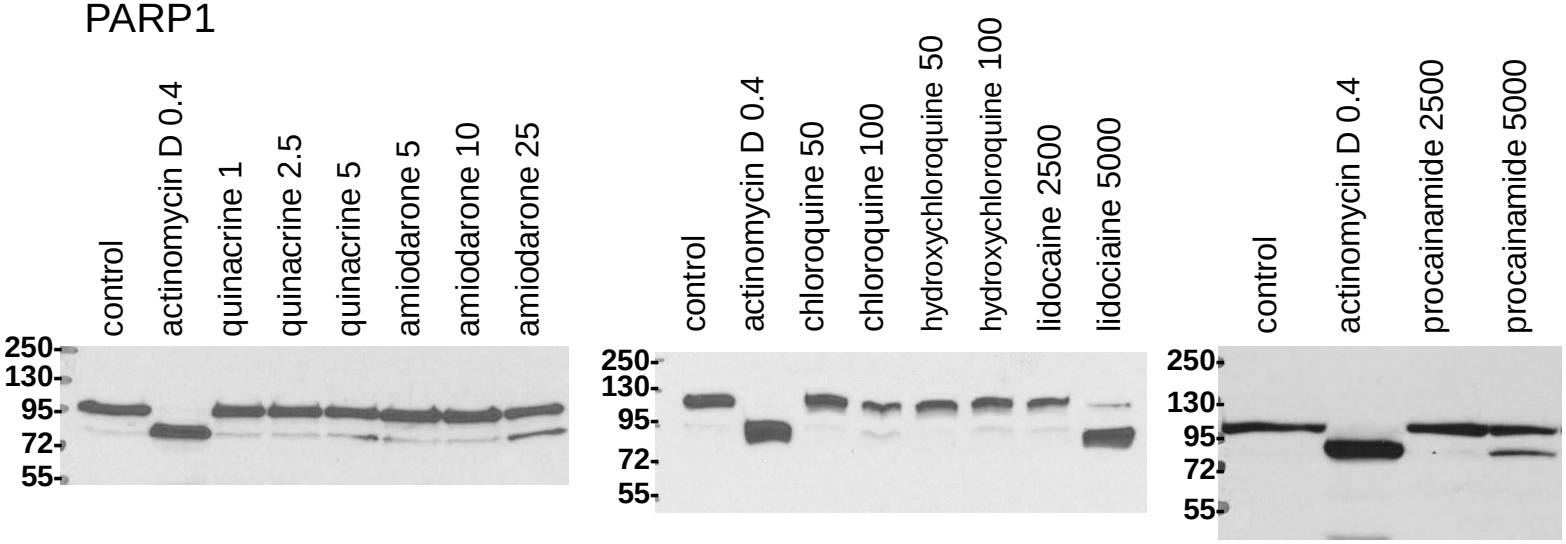

B.

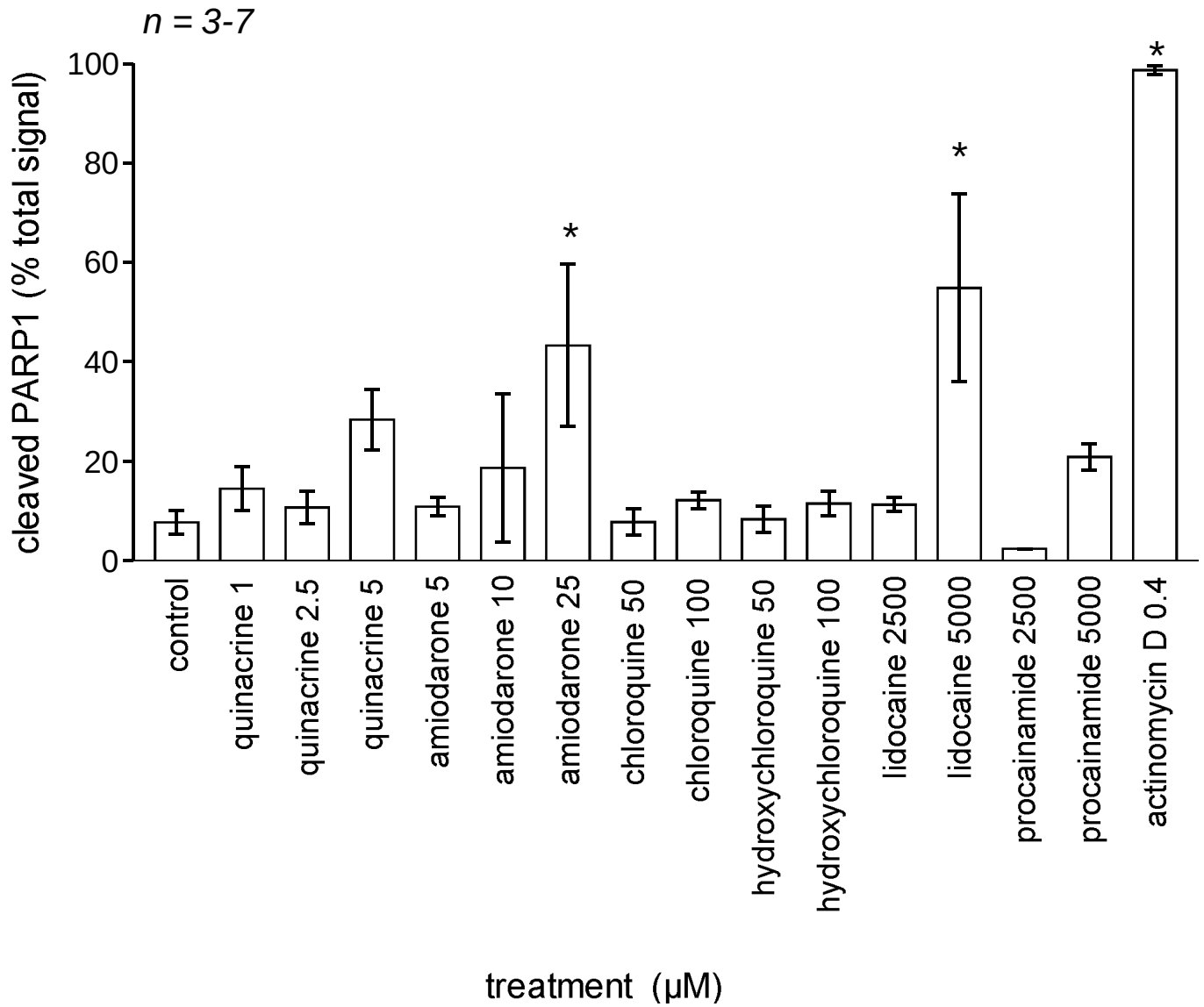

Figure 9

Fig. 9

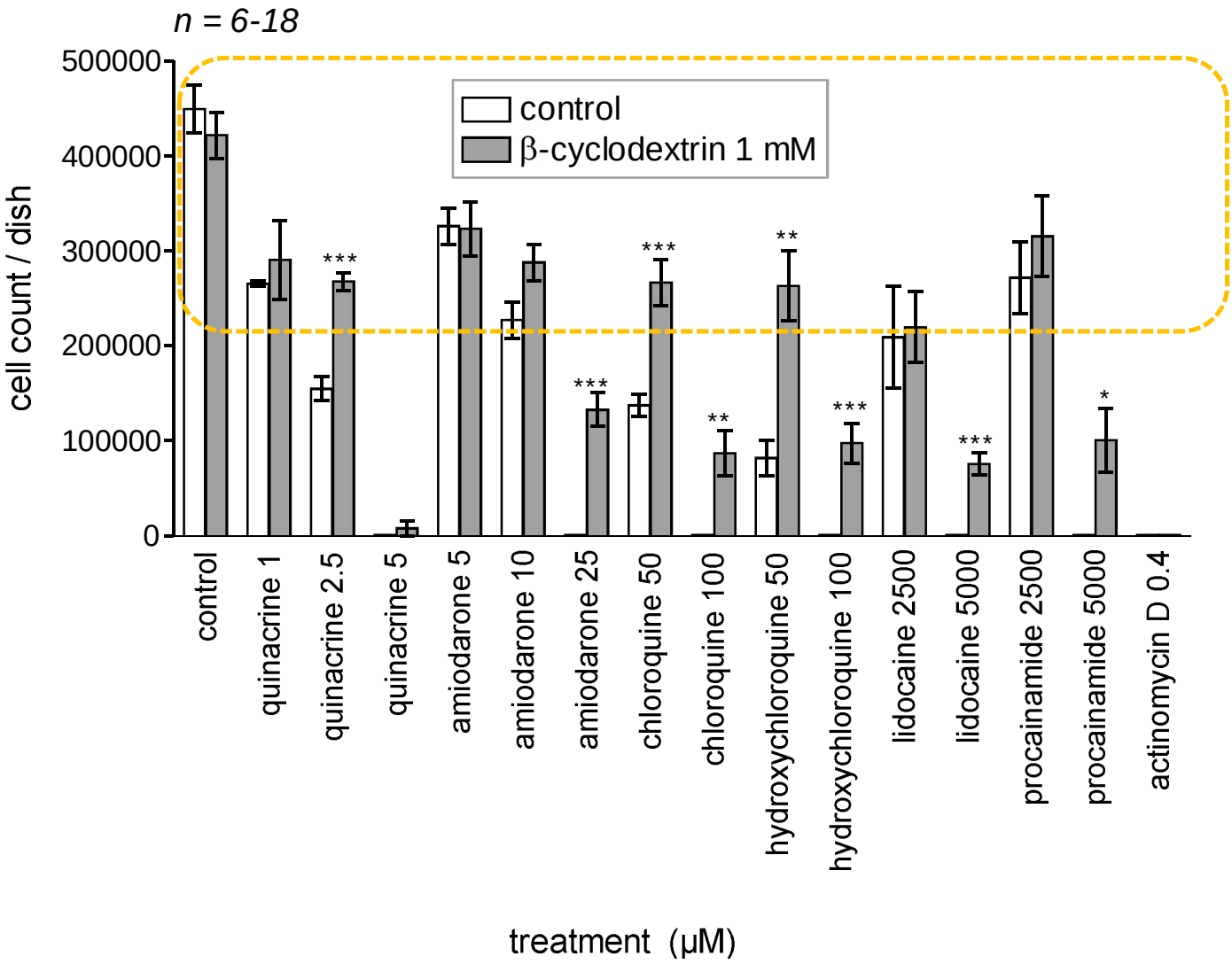

Figure 10

Fig. 10

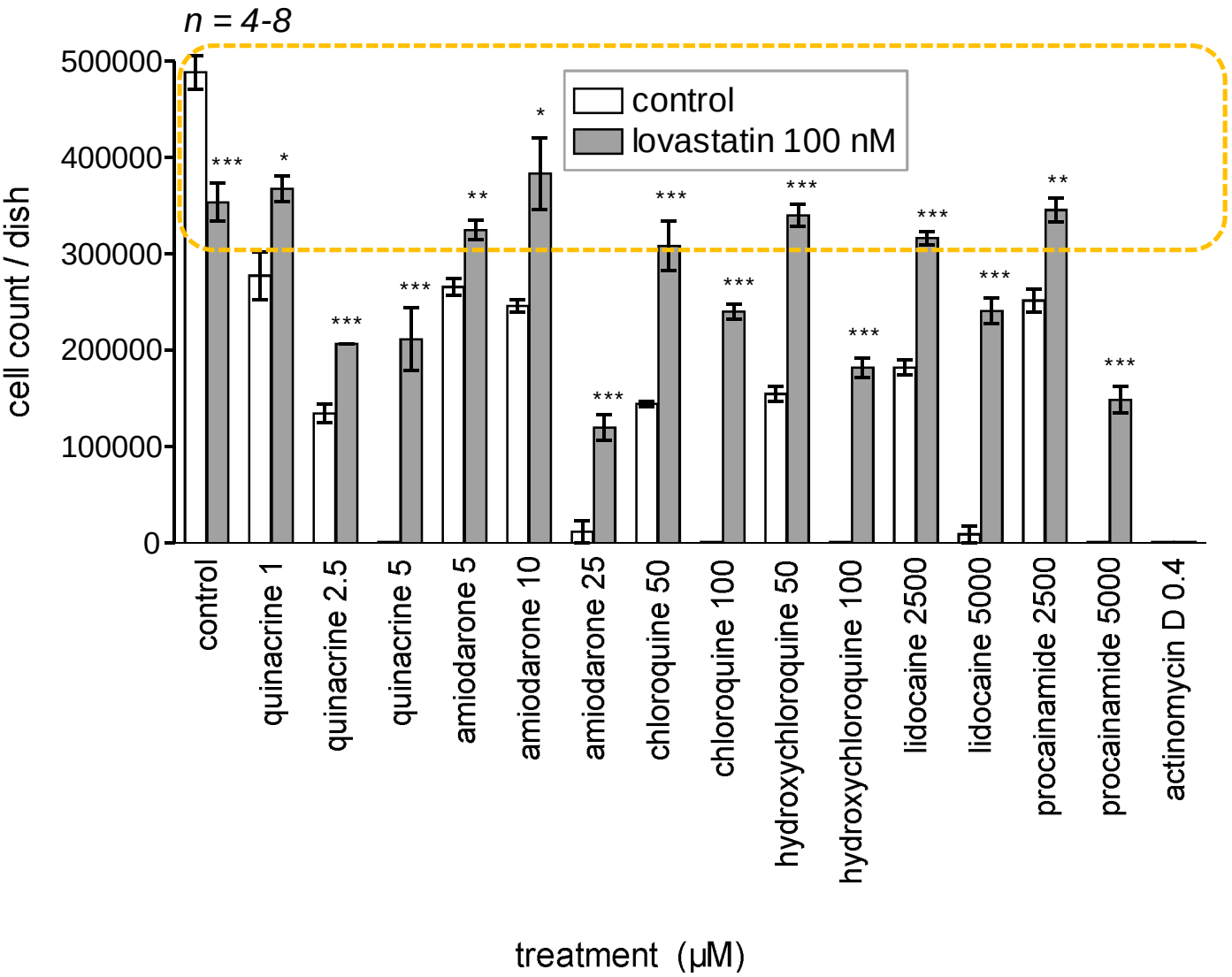

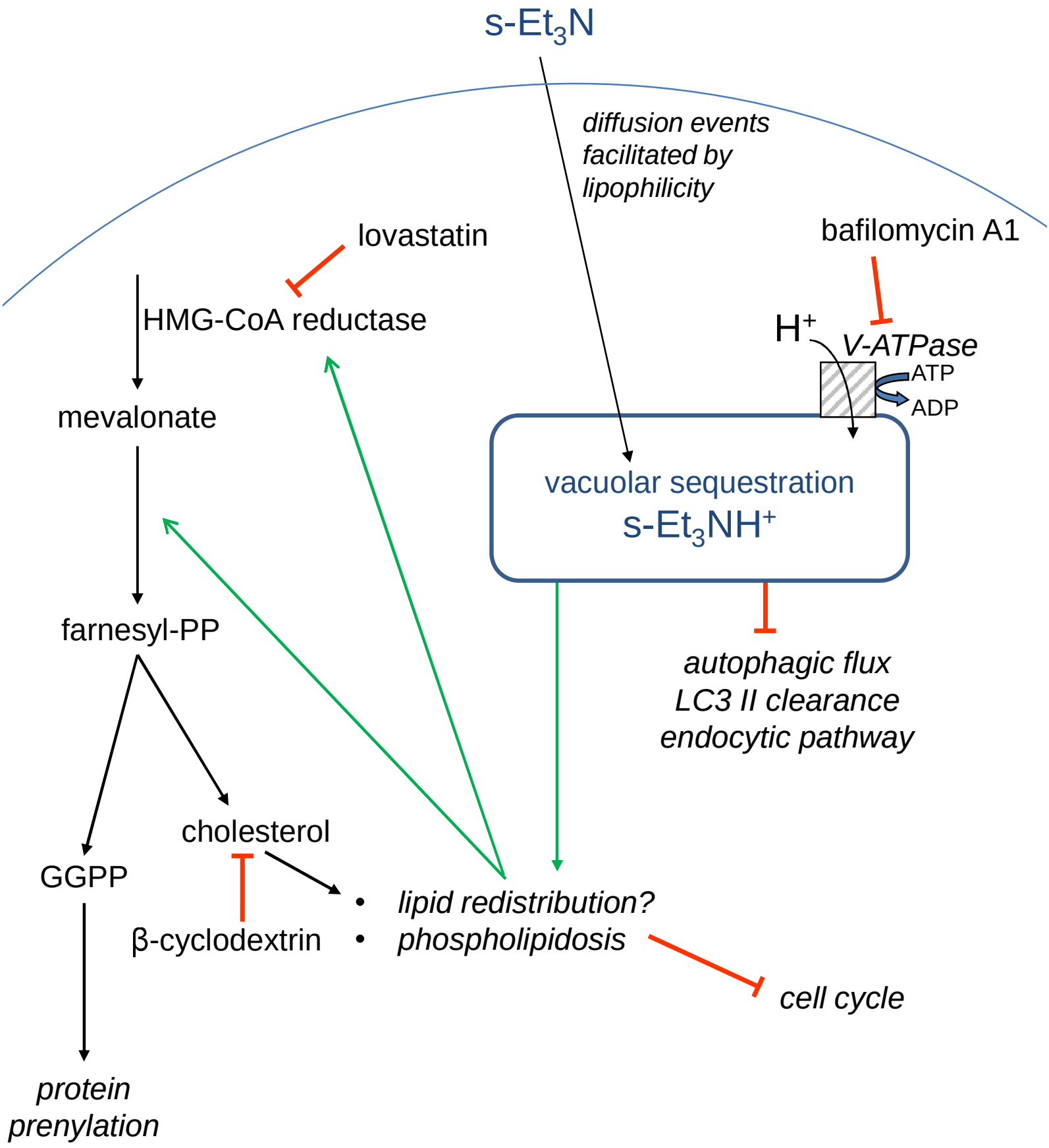
s-Et3N
diffusion events facilitated by lipophilicity
lovastatin
bafilomycin A1
HMG-CoA reductase
H+
V-ATPase
ATP
ADP
mevalonate
vacuolar sequestration
s-Et3NH+
farnesyl-PP
autophagic flux
LC3 II clearance
endocytic pathway
cholesterol
GGPP
β-cyclodextrin
• lipid redistribution?
• phospholipidosis
cell cycle
protein prenylation

Supplementary Material

Click here to download Supplementary Material: 1606-data supplement.pdf